JOINT INSTITUTE FOR NUCLEAR RESEARCH
Veksler and Baldin laboratory of High Energy Physics

FINAL REPORT ON THE START PROGRAMME

Modeling of processes with lepton flavor violation at CMS

Supervisor:
Dr. Sergei Shmatov

Student:
Uladzislau Yanuts, Belarus
Byelorussian State University

Participation period:
July 17 – August 27,
Summer Session 2022

Dubna, 2022

Contents

1 Introdution

There are a number of indications that the construction of the physical picture of the world is not complete: a large number of free parameters (the masses of quarks and leptons as an example), the lack of explanation of dark matter, neutrino oscillation, gravitational interaction, the origin of the Higgs mechanism, etc.

This has led to the emergence of many models whose predictive power needs to be tested empirically. This leads to the search for all sorts of deviations in SM, which tell us which way to move. One of these deviations is a violation of the lepton flavor.

The symmetry of the lepton flavor is accidental and it is broken by nonzero neutrino masses and mixing. In the case of charge leptons , lepton flavor violation is suppressed as $(m_\nu/m_W) \approx 10^{-48}$ [1]. This make LFV processes one of the main directions for the search of BSM physics. In this paper, we consider the process $pp \to e\mu$, the description of which is based on effective field theory. To describe this process, an effective Lagrangian is constructed, on the basis of which an effective differential cross-section of the process is derived, which can be used for computer modeling, which is actually performed in this work.

2 Project goals

The aim of the work is to estimate the number of processes with LFV on RUN3 and RUN4 on CMS. To do this, it is necessary to simulate in Monte Carlo generators in order to obtain LHE files for subsequent full simulation of the process in the detector using the capabilities of the CMSSW shell. At the next stage of the work, the intervals of physical quantities are searched in which signal events can be separated from the background and, in the case of the actual existence of the process, detected experimentally. After that, the project will move to the stage of statistical analysis, during which it will be possible to estimate the number of events and the possibility of separating the signal from the background.

3 Modeling of processes with lepton flavor violation

3.1 Features of finding the signal process

In order to detect signal events, we need to suppress background events. To do this, we need to identify the circle of these events, after which, during

the simulation of background and signal processes, we will be able to identify kinematic constraints that will allow us to simplify the search for a signal.

3.1.1 Signal process

To generate signal events, the differential cross section of our LFV process is used, obtained from the effective Lagrangian of the interaction in the work [1]:

$$\left[\frac{d\hat{\sigma}}{dt}\right]_{ijkl} = \frac{\left(\hat{s}+\hat{t}\right)^2}{48\pi v^4 \hat{s}^2} \times$$
$$\times \left\{ \left[|C_{V_{LL}}|^2 + |C_{V_{LR}}|^2 + (L \leftrightarrow R)\right] + \frac{\hat{s}^2}{4\left(\hat{s}+\hat{t}\right)^2}\left[|C_{S_L}|^2 + |C_{S_R}|^2\right] + \right.$$
$$\left. + \frac{4\left(\hat{s}+2\hat{t}\right)^2}{\left(\hat{s}+\hat{t}\right)^2}|C_T|^2 - \frac{2\hat{s}\left(\hat{s}+2\hat{t}\right)}{\left(\hat{s}+\hat{t}\right)^2}\,\mathrm{Re}\left(C_{S_L}C_T^*\right) \right\}, \quad (1)$$

In this work, the coefficients are also estimated based on the data obtained at LHC RUN2 on the ATLAS detector.

It is important to note that this differential cross-section is not associated with any specific physical model, but is a phenomenological expression for a four-particle interaction that allows to estimate the probability of an LFV process and its kinematics.

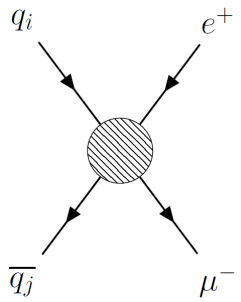

Figure 1: Diagram for the LFV process.

It is important to note that the modeling did not take into account the features of interaction with different flavors of quarks, which led to the asymmetry of the signal process by pseudorapidity.

3.1.2 Background processes

The main backgrounds for LFV-process are:

- The Drell-Yang process with the creation of a pair of τ-leptons with subsequent decay into leptons of various flavors.

- The process of $pp \to WW$ with subsequent decays into lepton-anti-neutrino (antilepton-neutrino) pairs of different flavors.

These processes are good backgrounds, because they are well studied. In particular, the Drell-Yang process is used to calibrate detectors and test event generators in HEP.

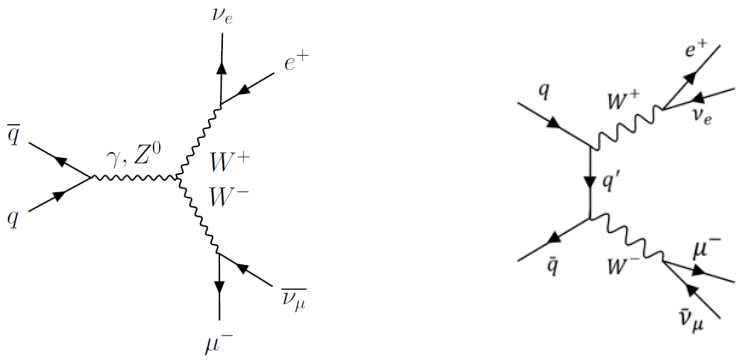

Figure 2: Diagrams of $pp \to WW$ process.

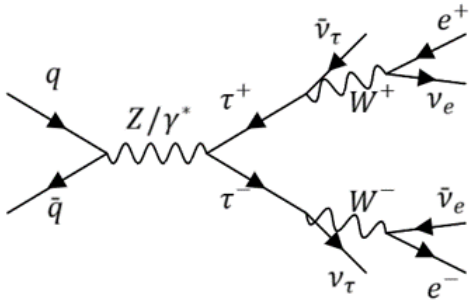

Figure 3: Diagram of the Drell-Yang process with the creation of a pair of τ-leptons.

3.2 Modeling methodology

The following software was used to simulate the processes under study

- Event Generator PYTHIA 8.307;
- MadGraph5 Event Generator;
- ROOT data processing package;
- Package for converting LHE files to ExRootAnalisis ROOT files.
- CMSSW v.12.4.5 shell for full simulation.

To take into account the conditions of the CMS experiment, we use the parameters of the processes that will be achieved during the current experiment session (RUN 3): the luminosity of 300 fb^{-1}, the particle collision energy (pp) $\sqrt{s}$ = 14TeV, and various input parameters for the cmsDriver tool.

3.2.1 PYTHIA 8.307

Background and signal events were generated in PYTHIA.

Background events are in the Pythia library by default.

The flag *WeakSingleBoson:ffbar2gmZ* was used to generate Drell-Yang processes, and *WeakDoubleBoson:ffbar2WW* was used for the process $pp \to WW$.

For simulation of signal process the capabilities of the *Sigma2Process* class are used, which allows one to create an inheritor class used when generating a user process. To create this class, it is necessary to know the incoming and outgoing particles, the interaction between quarks of different colors and knowledge of the differential cross section. It is extremely convenient to work with the particles formed during the simulation and record them in histograms. This is one of the reasons why Pythia was chosen to model the process. In addition, Pythia takes into account secondary processes and systematic effects.

3.2.2 MadGraph5

MadGraph5 is a tool for creating ME. In addition, MadGraph is used in this paper to compare the values obtained from this event generator with the results from Pythia. Due to the possibility of setting events up to finite particles, as well as the ability to put kinematic constraints on events before the actual generation itself. MadGraph was used as a source of background charts.

In MadGraph, LHE files are created, which are input parameters for the cmsDriver tool.

3.2.3 Tool cmsDriver and CMSSW shell

Tool cmsDriver is an application inside the CMMSW shell, necessary to create a configuration file, which is subsequently sent to cmsRun. The whole process of full simulation in the detector works according to the "black box" principle: we set only input files, specify boundary conditions, simulation parameters and stages, while inside CMSSW there is a complex chain of interaction of other program structural units (Geant4, FastJet, etc.). At the output after the complete simulation chain, we get the output ROOT file, which we can analyze using the capabilities provided by the CMSSW shell.

3.3 Result of modelling

Based on the simulation results , histograms of distributions for the following values are constructed:

- lepton pairs Invariant mass $m_{inv} = \sqrt{(E_1 + E_2)^2 - (\mathbf{p_1} + \mathbf{p_2})^2}$,
- transverse momentum lepton pair $p_T = \sqrt{(p_x)^2 + (p_y)^2}$,
- transverse momentum of one lepton p_T,
- pseudorapidity η of muons and electrons $\eta = -ln\left[tg(\frac{\theta}{2})\right]$,
- azimuthal angle φ between the outgoing electrons and muons.

3.3.1 Comparison of background processes

The figures below show the distributions of events modeled in MadGraph and Pythia generators of various kinematic characteristics. The diagrams 4,5,**??**show background processes for comparison.

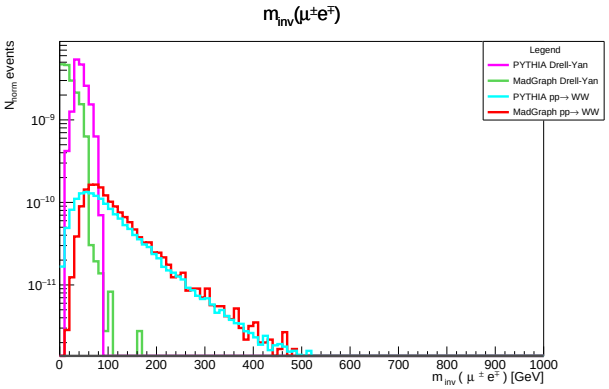

Figure 4: Invariant mass distribution of lepton pair.

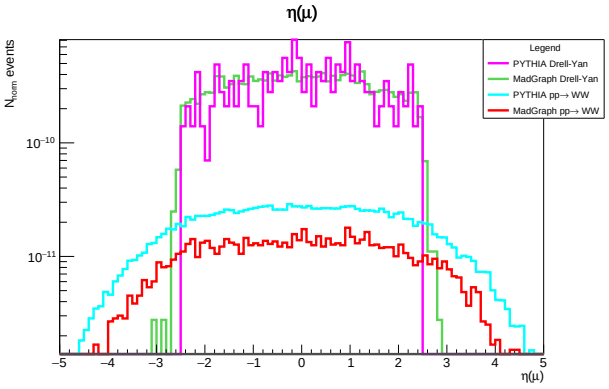

Figure 5: Pseudorapidity distribution of muons.

It is important to pay attention to the ratio of Drell-Yang backgrounds and $pp \to WW$. At first glance, the main background for our signaling process is the Drell-Yang process. However, the graphs below will show that this is not the case.

3.3.2 Signal process

After generating the signal process in Pythia, histograms of the following type are obtained:

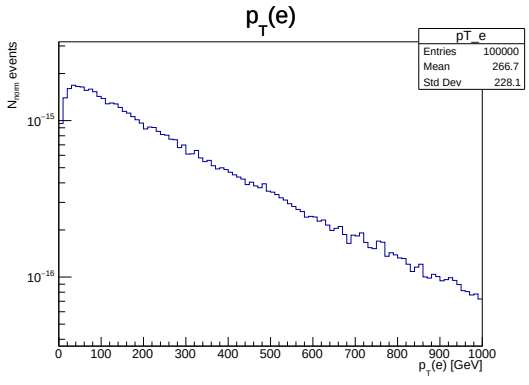

Figure 6: Transverse momentum distribution of muons

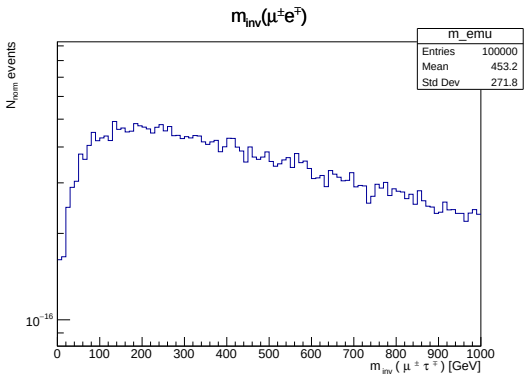

Figure 7: Invariant mass distribution of lepton pair.

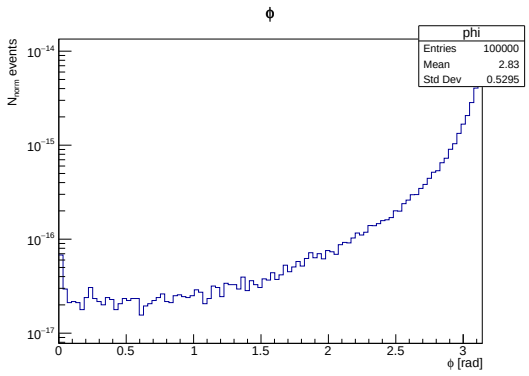

Figure 8: Azimuth angle distribution of lepton pair.

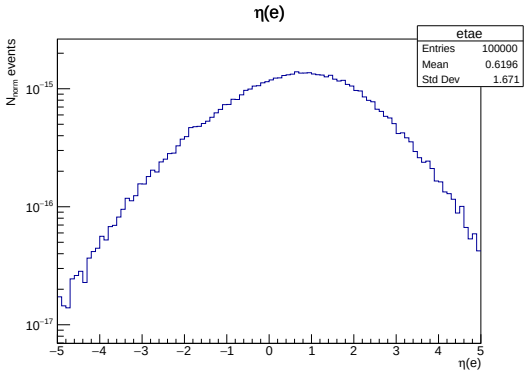

Figure 9: Pseudorapidity distribution of electrons.

To better demonstrate the need to impose kinematic constraints, we compare histograms of the LFV of the process multiplied by a factor of 10^5 and background histograms.

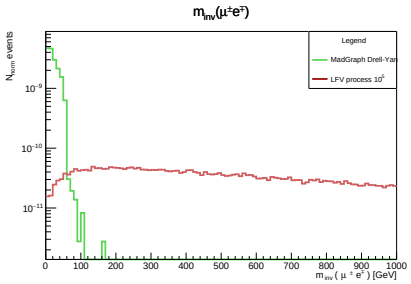

Figure 10: Comparison of invariant mass distributions of lepton pair for the DY process and the signal.

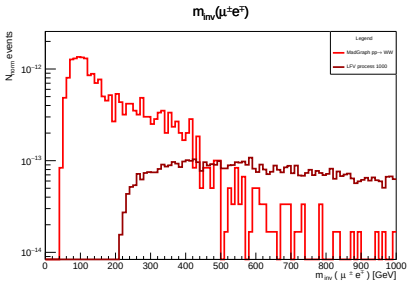

Figure 11: Comparison of invariant mass distributions of lepton pair for the WW process and the signal.

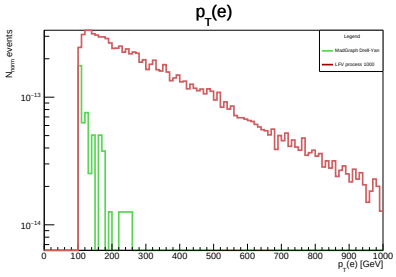

Figure 12: Comparison of transverse momentum distributions of electrons for the DY process and the signal.

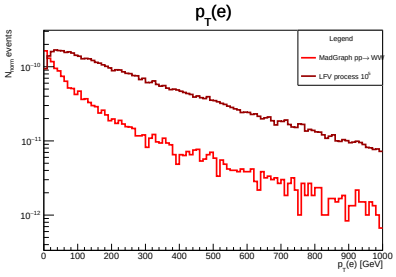

Figure 13: Comparison of transverse momentum distributions of electrons for the WW process and the signal.

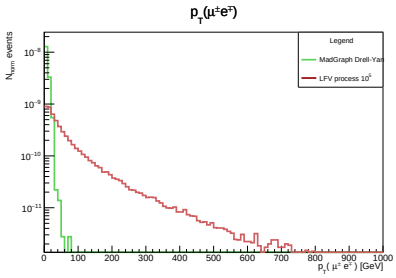

Figure 14: Comparison of transverse momentum distributions of lepton pair for the DY process and the signal.

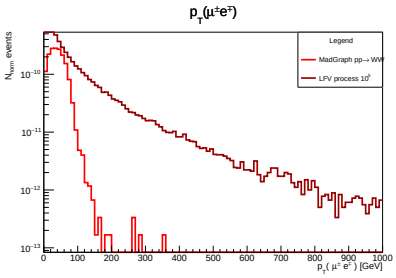

Figure 15: Comparison of transverse momentum distributions of lepton pair for the WW process and the signal.

After analyzing the histograms, the following kinematic constraints were selected:

- Restriction on the transverse momentum of the lepton $p_T(lepton) > 100$ GeV,

- Restriction on the pseudo-speed of the lepton $|\eta(lepton)| < 2.5$,
- Restriction on the total transverse momentum of a pair of leptons $p_T(e\mu) < 30$ GeV.

3.3.3 Imposition of kinematic restrictions

The diagrams 16, 17, 18, 19 compare backgrounds and signal with imposed restrictions.

It is worth paying attention to the diagrams 16,17, where the coefficient for the signal process, due to the imposition of kinematic restrictions, decreased by 2 orders of magnitude and practically suppressed the Drell-Yang background. On 18,19 diagrams it can be seen that the process plays a key role in detecting the signal $pp \to WW$.

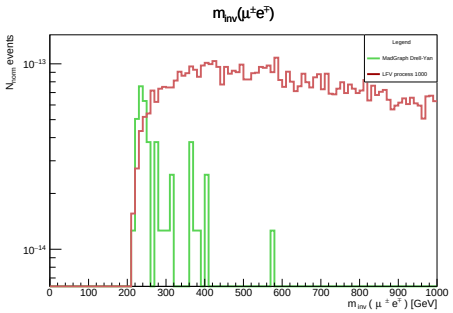

Figure 16: Comparison of invariant mass distributions of lepton pair for the DY process and the signal.

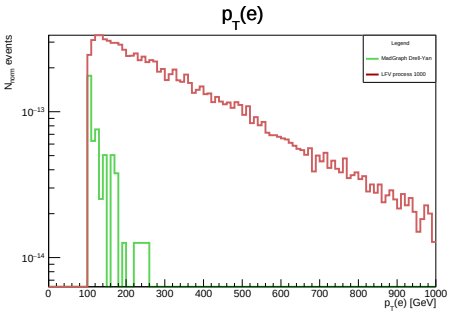

Figure 17: Comparison of transverse momentum distributions of electrons for the DY process and the signal.

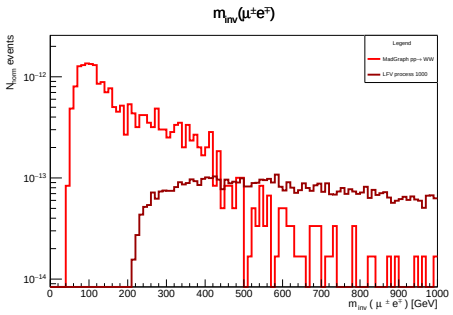

Figure 18: Comparison of invariant mass distributions of lepton pair for the WW process and the signal.

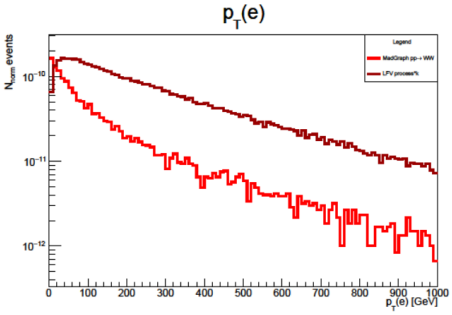

Figure 19: Comparison of transverse momentum distributions of electrons for the WW process and the signal.

Based on the diagrams and the type of distribution of our process, it is good idea to imposing another kinematic restriction to suppress the background from WW and the Drell-Yang process:

$$m_{inv}(e\mu) < 30\,GeV$$

After applying these restrictions, the diagrams look as shown in the diagrams 20, 21, 22, 23.

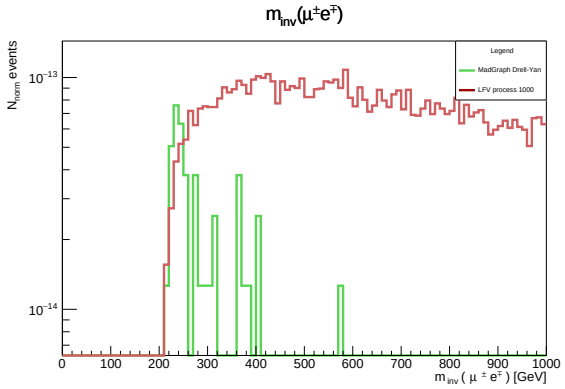

Figure 20: Comparison of invariant mass distributions of lepton pair for the DY process and the signal.

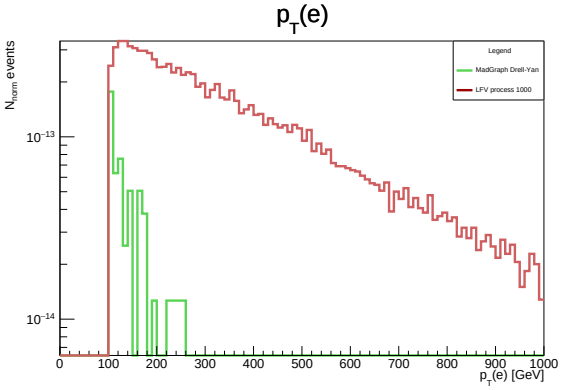

Figure 21: Comparison of transverse momentum distributions of electrons for the WW process and the signal.

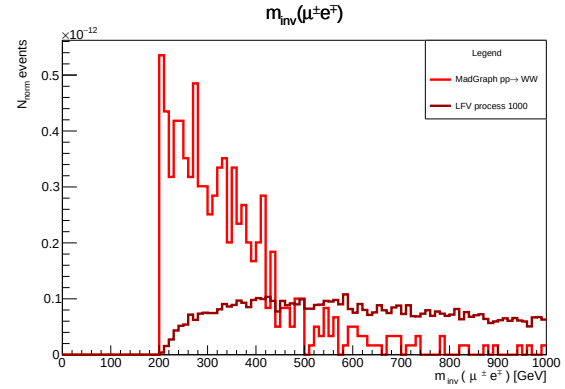

Figure 22: Comparison of invariant mass distributions of lepton pair for the WW process and the signal.

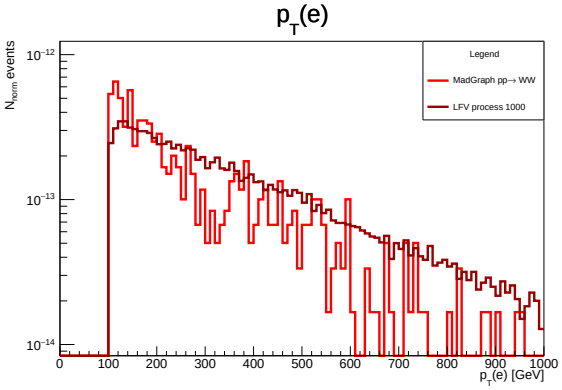

Figure 23: Comparison of transverse momentum distributions of electrons for the WW process and the signal.

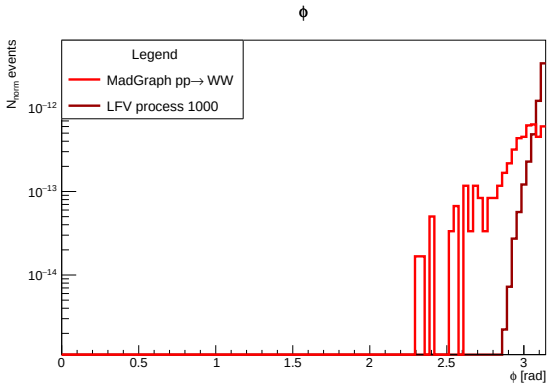

Figure 24: Comparison of angle distributions between outgoing leptons for the WW process and the signal.

A complete simulation in the detector shows that the Drell-Yang process can be completely suppressed. There are also considerations about greater suppression of the $pp \to WW$ process, which will be checked after a full simulation in the detector.

4 Conclusion

During the execution of the work to detect the LFV process the following kinematic constraints were made:

- Restriction on the transverse momentum of the one lepton $p_T(lepton) > 100$ GeV,
- Restriction on the pseudo-speed of the one lepton $|\eta(lepton)| < 2.5$,
- Restriction on the total transverse momentum of a pair of leptons $p_T(e\mu) < 30$ GeV,
- Restriction on the invariant mass of a pair of leptons $m_{inv}(e\mu) > 200$ GeV.

The main background preventing our signaling process from being detected is the $pp \to WW$ process, which begins to dominate when all of the above cuts are applied, and not the Drell-Yang process, as it might seem at first glance.

Here is what the cross sections of our processes look like at the output after generation with all the kinematic constraints established during the study

- Drell-Yang: $\sigma = 4.41438 \cdot 10^{-13}$ mb,
- $pp \to WW$: $\sigma = 8.61698 \cdot 10^{-12}$ mb,

- LFV process: $\sigma = 1.096 \cdot 10^{-14}$ mb.

The connection of the average number of events, luminosity and total cross-section:

$$N = L\sigma \tag{2}$$

In RUN3 LHC, a luminosity of 300 fb^{-1} is expected. In this case, about 10 events are expected. If we take into account the expected luminosity of RUN3 and RUN4 (3000 fb^{-1}), we are already getting 97 events. Considering that the Higgs boson was found at a dozen events — this process is quite realistic to detect in an experiment.

The first results after a full simulation in the detector say that the Drell-Yang background can be completely suppressed. In the future, the analysis of the process will be completed after passing through the detector, after which it is planned a statistical analysis.

References

[1] Angelescu, Andrei and Faroughy, Darius A. and Sumensari, Olcyr, Lepton Flavor Violation and Dilepton Tails at the LHC // Eur. Phys. J. C. – 2020. – Vol.80. – N. 7. – P. 641.

[2] .A. Zyla et al. (Particle Data Group) // Prog. Theor. Exp. Phys. – 2020. –P. 083C0.